

# Determination of Pavement Layer Thicknesses and Moduli by SASW Method

SOHEIL NAZARIAN, KENNETH H. STOKOE II, ROBERT C. BRIGGS, AND RICHARD ROGERS

Nondestructive tests are being used more than ever in evaluating the integrity of existing pavement systems. The nondestructive tests can be divided into two main categories: (1) deflection-based methods, in which devices such as the Falling Weight Deflectometer (FWD) and dynaflect are used, and (2) wave propagation methods such as the Spectral-Analysis-of-Surface-Waves (SASW) method. The SASW method has several significant advantages over deflection-based methods. One advantage is that moduli of thin pavement layers in the upper portion of the pavement system can be easily and accurately measured. A second advantage is that variations in moduli within different layers, especially in the lower portions of the base and in the subgrade, can be evaluated. This feature is particularly beneficial when bedrock is close to surface. A third advantage is that layering in the pavement system does not have to be known. In fact, the thickness of the layers can be determined as illustrated in the modulus profiles presented in the paper. A series of tests was performed at nine flexible pavement sections with significantly different profiles to evaluate the accuracy of layer thickness determination by the SASW method. The thicknesses of the asphaltic-concrete surface layer varied between 1 and 5 inches. The base and subbase materials consisted of substantially different materials. No information regarding the types or thicknesses of the layers was provided during data collection or reduction. Only after the results were reported to the Texas State Highway Department were the pavement profiles known. It was found that the SASW method predicted the thicknesses of the layers quite closely. In addition, moduli determined by the SASW method were compared with moduli back-calculated from FWD tests performed at the same sites. The variation in moduli of similar materials used at different sections exhibit somewhat less scatter when obtained from SASW tests. However similar trends were found with both methods.

The Spectral-Analysis-of-Surface-Waves (SASW) method is a field seismic method for determining moduli and thicknesses of pavement systems. As with any in situ method, limitations in terms of accuracy in the final modulus profiles should be understood. The sources of these limitations can be varied. For instance, limitations can result from--

- The degree of sensitivity of the parameter being measured to the moduli,

S. Nazarian, Department of Civil Engineering, The University of Texas, El Paso, Tex. K. H. Stokoe, II, Geotechnical Engineering, The University of Texas, Austin, Tex. R. C. Briggs and R. Rogers, Pavement Management Section, Texas Department of Highways and Public Transportation.

- The amount of simplification introduced in the theoretical model used for data reduction,
- The degree to which the field data collection deviates from the assumptions made in developing the theoretical model,
- Inevitable scatter in the data collected in the field, and
- Any dependency of the method on personnel skills in data collection and/or reduction.

To better understand the limitations of the SASW method, a series of theoretical, parametric, and sensitivity studies, as well as extensive field investigations, have been conducted at The University of Texas during the last several years. This paper presents the results of one of the field studies.

The SASW method was used at nine sites at the Pavement Test Facility of Texas A&M University in Bryan, Texas, in March 1986. The primary objective of the tests was to evaluate the effectiveness of the SASW method in determining the thicknesses of various layers of different materials comprising the pavement systems. A secondary objective was to study moduli variations in similar materials at carefully controlled pavement sites. The results are reported herein, along with brief background information on the SASW method and an explanation of the procedures and data analyses. In addition, moduli obtained from FWD tests performed on the same sections are included for comparison purposes.

It should be noted that no information pertaining to the types of materials or thicknesses of the layers was provided at the time of testing or data reduction (except for Site 7). The material profiles reported herein were provided after Young's modulus profiles of the different sites were reported to the Texas State Department of Highways and Public Transportation.

## SPECTRAL-ANALYSIS-OF-SURFACE-WAVES TESTING

### General Background

The Spectral-Analysis-of-Surface-Waves (SASW) method is a method of seismic testing developed for determining small-strain Young's modulus profiles at pavement sites and small-strain shear modulus profiles at soil sites (1, 2). The SASW method is a nondestructive method in which both the source and receivers are located on the pavement surface. The source is simply a transient vertical impact that generates surface waves of various frequencies, which the medium transmits. Two vertical receivers, located on the surface, monitor the

propagation of surface wave energy past them. By analysis of the phase information of the cross power spectrum for each frequency determined between the two receivers, phase velocity, shear wave velocity, and elastic moduli are determined.

The terms elastic or small-strain are generally used to describe moduli evaluated by SASW testing. These terms are used (or their use is implied) because stress waves generated in this type of seismic testing create strains in the medium that are less than 0.001 percent. Moduli measured at these strain levels are essentially constant and, hence, independent of strain amplitude (3, 4). Therefore, the medium being tested behaves like an elastic material. This low stress level also allows for truly nondestructive testing.

Two key points in SASW testing are the generation of primarily first-mode surface wave energy and the measurement of surface waves (Rayleigh waves) at significant distances from the source. Rayleigh wave velocity,  $V_R$ , is constant in a homogeneous half-space and independent of the frequency. Each frequency,  $f$ , has a corresponding wavelength,  $L_R$ , according to:

$$V_R = fL_R \quad (1)$$

Rayleigh wave and shear wave velocities are related by Poisson's ratio. In an isotropic elastic half-space, the ratio of Rayleigh-wave-to-shear-wave velocity increases as Poisson's ratio increases. This ratio varies from 0.90 to 0.96 for values of Poisson's ratio ranging from 0.15 (concrete) to 0.5 (saturated subgrade).

If the stiffness of a site varies with depth, then the velocity of the Rayleigh wave (R-wave) will vary with frequency. The variation of R-wave velocity with frequency (wavelength) is called dispersion. The dispersive characteristic of surface waves is the key to the SASW method. A plot of surface wave velocity versus wavelength is called a dispersion curve. The dispersion curve is developed from phase information of the cross power spectrum. This information provides the relative phase between two signals (two-channel recorder) at each frequency in the range of frequencies excited in the SASW test. For a travel time equal to one period of the wave, the phase difference is 360 degrees. Thus, for each frequency the travel time between receivers can be calculated by

$$t(f) = \phi(f)/(360f) \quad (2)$$

where:

- $f$  = frequency,
- $t(f)$  = travel time for a given frequency, and
- $\phi(f)$  = phase difference in degrees for a given frequency

The distance between the receivers,  $D$ , is a known parameter. Therefore, R-wave velocity at a given frequency,  $V_R(f)$ , is simply calculated by

$$V_R(f) = D/t(f) \quad (3)$$

and the corresponding wavelength of the R-wave is equal to

$$L_R(f) = V_R(f)/f \quad (4)$$

By repeating the procedure outlined by equations 2 through 4 for every frequency, the R-wave velocity corresponding to each wavelength is evaluated, and the dispersion curve is determined. Several studies have been performed recently to evaluate the optimum source/receiver array. The general array

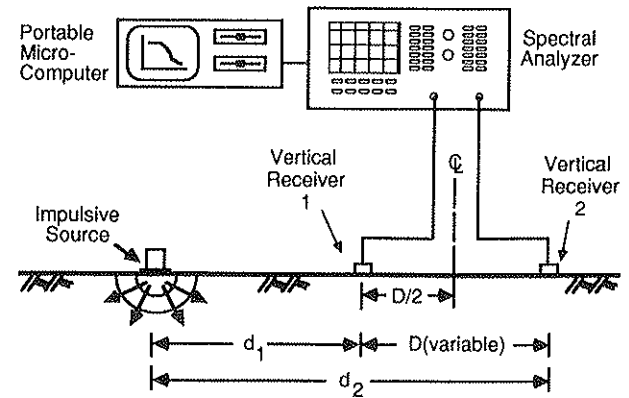


FIGURE 1 General configuration of SASW testing.

configuration is shown in figure 1. The distances are expressed as follows: source to near receiver =  $d_1$ , source to far receiver =  $d_2$ , and receiver to receiver =  $D$ . Analytical studies by Sanchez-Salinerio (5) show that a desirable array configuration can be expressed as:

$$d_2/d_1 = 2 \quad (5)$$

Sheu et al. (6) combined experimental studies on pavements with the analytical work of Sanchez-Salinerio (5) to determine the range of wavelengths that can be accurately obtained with a fixed source/receiver spacing. They found that for an array with  $d_2/d_1 = 2$  the distance between receivers can be related to useable wavelengths as

$$L_R < 3D \quad (6)$$

As the velocities of different layers are unknown before testing, it is difficult to know if the limit expressed in equation 6 is satisfied. Practically speaking, it is more appropriate to test with various distances between the receivers in the field and then evaluate the range of wavelengths over which reliable measurements were made. The procedure is to select a spacing between receivers, perform the test, and reduce the data to determine the wavelengths and associated velocities. The next step is to eliminate the points that do not satisfy equation 6.

Rayleigh wave velocities determined by this method are not actual velocities of the layer, but apparent R-wave velocities (known as phase velocities). Existence of a layer with high or low velocity at the surface of the medium affects measurement of the velocities of the underlying layers. Therefore, a method for distinguishing shear-wave velocities from phase velocities is necessary in SASW testing.

Inversion of the dispersion curve, or (in short) inversion, is the procedure of determining the shear-wave velocity profile from the dispersion curve. Inversion consists of determination of the depth of each layer and the actual shear-wave velocity of each layer from the apparent R-wave velocity versus wavelength information.

The inversion process used herein is based on a modified version of Thomson's (7) and Haskell's (8) matrix solution for elastic surface waves in a layered solid media. To simplify the process of inversion, some assumptions were made. These assumptions include—

- The layers are horizontal,

- The velocity of each layer is constant, and
- The layers are homogeneous and linearly elastic.

The inversion process is an iterative process in which a shear-wave velocity profile is assumed and a theoretical dispersion curve is constructed. The experimental and theoretical dispersion curves are compared and necessary changes are made in the assumed shear-wave velocity profile until the two curves (experimental and theoretical dispersion curves) match within a reasonable tolerance.

Once the shear-wave velocities are determined, the following formulae are used to calculate shear and Young's moduli:

$$G = \rho V_s^2 \tag{7}$$

and

$$E = 2G(1 + \nu) \tag{8}$$

where

- $G$  = shear modulus
- $E$  = Young's modulus
- $\rho$  = mass density and
- $\nu$  = Poisson's ratio

As mentioned earlier, moduli obtained in this manner are the elastic, or small-strain, moduli. A methodology to account for non-linear behavior of moduli obtained for different layers utilizing the SASW method is suggested by Nazarian et al. (9). This methodology is the same as that employed in geotechnical earthquake engineering where small-strain moduli evaluated by in situ seismic tests are adjusted to values appropriate for large-strain earthquake excitation by combining (linear) field and (nonlinear) laboratory moduli.

**Field Procedure**

The general configuration of the source, receivers, and recording equipment is shown in figure 1. Accelerometers were used as receivers for close receiver spacings ( $\leq 4$  feet), and geophones with a natural frequency of 4.5 Hz were used as receivers for greater spacings. This was done to optimize recording of the wave passage; that is, accelerometers produce more output

at closer receiver spacings where high frequencies are present, while geophones produce more output at larger receiver spacings where low-frequency R-waves are excited.

The common receivers midpoint (CRMP) geometry (10) was used for testing. With this geometry the two receivers were each moved an equal distance away from an imaginary center line between the receivers, and the source was moved so that the distance between the source and near receiver was equal to or greater than the distance between the two receivers. In addition, the location of the source was reversed for each receiver spacing so that forward and reverse profiles were run. This testing sequence is illustrated in figure 2. Distances between receivers of 0.5, 1, 2, 4, and 8 feet were used at each site.

Different sources were used. For close receiver spacings, a 4-oz hammer was used. For greater distances, 2.5- and 5-lb sledge hammers were employed, with the largest hammer generally used at the 8-ft spacing.

The recording device was a Hewlett-Packard 3562A Fourier spectral analyzer. This analyzer is a digital oscilloscope combined with a micro-processor that can perform directly in either the time or the frequency domain.

It is worthwhile noting here that the field procedure outlined above results in the performance of essentially two tests, one for the forward profile and one for the reverse profile. The results (in terms of dispersion curves) are typically very close, so that an average dispersion curve is calculated from the forward and reverse tests. One can think of this type of testing as a 1-test run at each site for the SASW method. However, the SASW method is very repeatable at the same site, with typically less than a five percent scatter among three or more tests (6, 11). Therefore, duplicate SASW tests were not performed in this study.

**PRESENTATION OF RESULTS**

**Description of Sites**

The general layout of the pavement test facility constructed at Texas A&M University in the mid-1960s is shown in figure 3. This facility, which is 460-ft long and 50-ft wide, consists

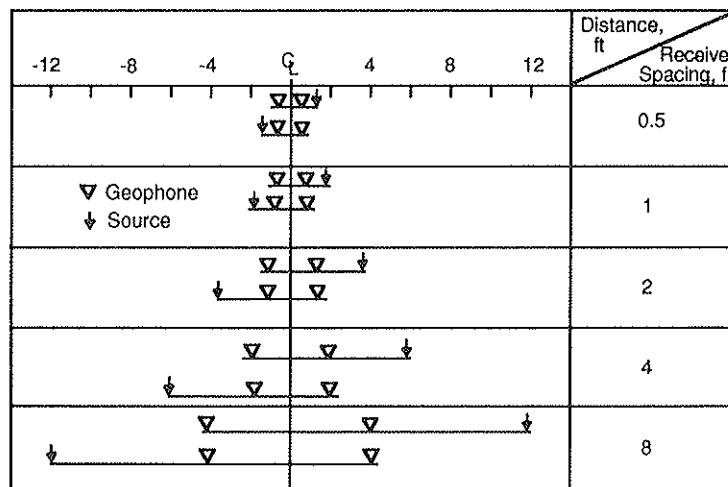
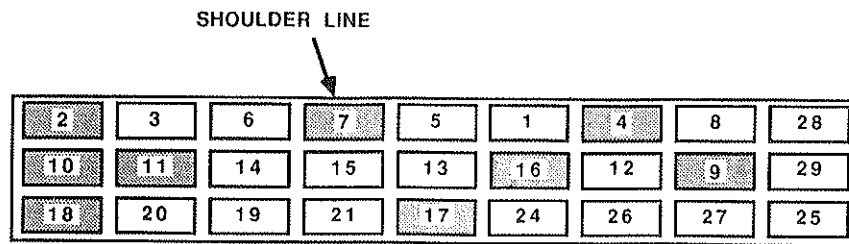


**FIGURE 2** Schematic of experimental arrangement for SASW tests.



SASW Tests were Performed at the Nine Highlighted Sections (Nos. 2, 4, 7, 9, 10, 11, 16, 17 and 18).

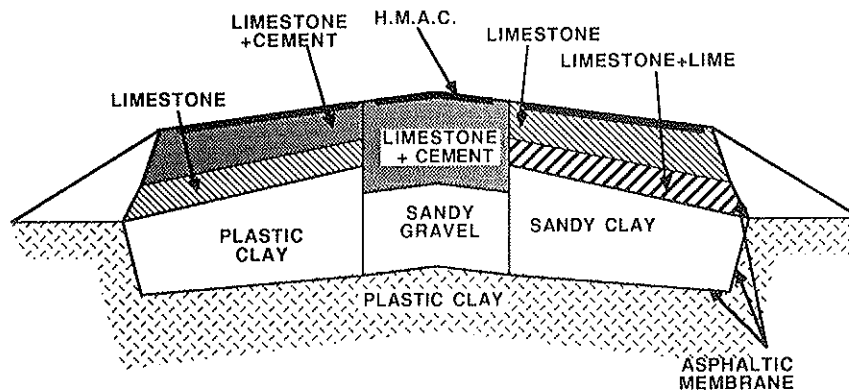


FIGURE 3 General layout of pavement test facility at Texas Transportation Institute.

TABLE 1 MATERIAL PROFILES OF TTI PAVEMENT TEST FACILITY (12)

Section	Thickness (in.)				Material Type			
	Surface	Base	Subbase	Embank.	Surface	Base	Subbase	Embank.
2	1	12	4	36	AC	LS+C	LS	PC
4	5	12	12	24	AC	LS+C	LS	PC
7	1	4	12	36	AC	LS	LS+C	PC
9	5	4	4	40	AC	LS	LS	GR
10	1	12	4	36	AC	LS	LS	GR
11	1	4	12	36	AC	LS	LS	GR
16	5	12	12	24	AC	LS+C	LS+C	GR
17	3	8	8	34	AC	LS+L	LS+L	SC
18	1	8	8	36	AC	LS+L	LS+L	SC

AC: Hot Mix Asphaltic Concrete  
 LS+C: Crushed Limestone mixed with 4% Cement  
 LS+L: Crushed Limestone mixed with 2% Lime

LS: Crushed Limestone  
 GR: Sandy Gravel  
 SC: Sandy Clay  
 PC: Plastic Clay

of 27 different pavement sections. Each section is approximately 40-ft long and 12-ft wide. Some of the sections in the facility do not represent typical pavement sections encountered on roads, since the main function of the facility was to determine the limitations and versatility of nondestructive testing methods.

Nine randomly selected sections were tested in March 1986. The nine sections are marked in figure 3. Material profiles of all sections, as reported by Scrivner and Michalak (12), are included in table 1. The top layer is always asphaltic-concrete pavement. Base and subbase materials are either crushed limestone or a mixture of crushed limestone with lime or

TABLE 2 ENGINEERING PROPERTIES OF MATERIALS USED IN CONSTRUCTION OF TTI PAVEMENT FACILITY (12)

Description	Abbreviation Used In Table 1	AASHO Class	Unified Soil Class	Texas Triaxial Class	Compressive Strength (psi)*
Plastic Clay	PC	A-7-6(20)	CH	5.0	22
Sandy Clay	SC	A-2-6(1)	SC	4.0	40
Sandy Gravel	GR	A-1-6	SW	3.6	43
Crushed Limestone	LS	A-1-a	GS-GM	1.7	165
Crushed Limestone + 2% Lime	LS+L	A-1-a	GW-GM	1.0	430
Crushed Limestone + 4% Cement	LS+C	A-1-a	GW-GM	1.0	2270
Hot Mix Asphalt Concrete	AC				

\*By Texas triaxial procedure at a lateral pressure of 5 psi

Note: The natural material below the embankments was plastic clay similar to that described above, changing to a denser clay at a depth of about 90 inches below the surface of the pavement. The dense clay is abbreviated DC; its properties were not determined in the laboratory.

cement. Subgrade materials consist of three different sands or clays. Engineering properties of each material determined by laboratory tests are given in table 2.

profiles at each site.) Spectral analysis functions measured at these sites are not presented for the sake of brevity. Typical functions can be found in Nazarian and Stokoe (2). However, the quality of the data collected in the field was very good.

**Dispersion Curves**

Typical dispersion curves from SASW testing at two of the nine sites (Sites 4 and 11) are shown in figures 4 and 5. (These curves represent the average values for the forward and reverse

**Shear-Wave Velocities**

Typical shear-wave velocity profiles after inversion of the dispersion curves are given in tables 3 and 4 for sites 4 and 11,

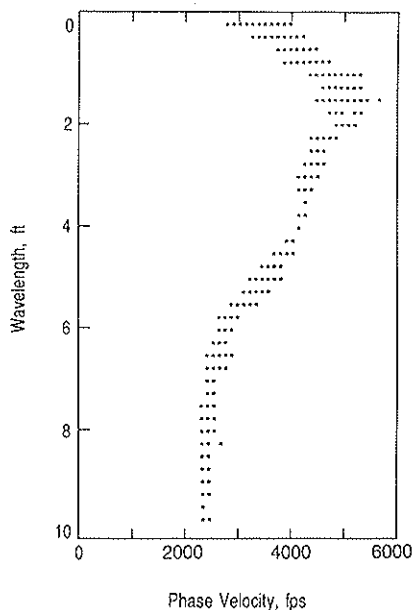


FIGURE 4 Dispersion curve from SASW tests at section 4.

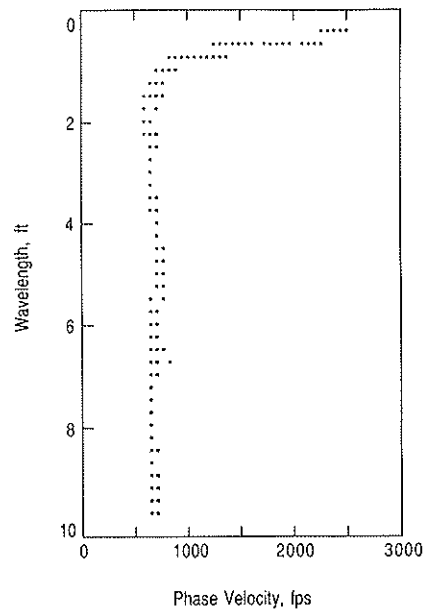


FIGURE 5 Dispersion curve from SASW tests at section 11.

TABLE 3 VARIATION OF SHEAR-WAVE VELOCITY AND YOUNG'S MODULUS WITH DEPTH AT SECTION 4

Layer Number	Layer Thickness	Layer Depth <sup>1</sup>	Shear Wave Velocity	Young's Modulus	Assumed Poisson's Ratio	Assumed Total Unit Weight
	in.	in.	fps	ksi		pcf
1	1.20	0.60	2239	337.9	0.25	125
2	1.20	1.80	2239	337.9	0.25	125
3	1.20	3.00	2239	337.9	0.25	125
4	1.20	4.20	2508	421.2	0.15	135
5	1.20	5.40	6261	2625.0	0.15	135
6	1.20	6.60	7115	3390.0	0.15	135
7	2.40	8.40	7115	3390.0	0.15	135
8	2.40	10.80	7115	3390.0	0.15	135
9	2.40	13.20	7115	3390.0	0.15	135
10	2.40	15.60	7043	3322.0	0.15	135
11	2.40	18.00	3005	604.7	0.15	135
12	2.40	20.40	2757	509.1	0.15	135
13	4.80	24.00	2757	509.1	0.15	135
14	4.80	28.80	2757	509.1	0.15	135
15	4.80	33.60	1366	125.8	0.25	125
16	4.80	38.40	1335	120.1	0.25	125
17	4.80	43.20	1333	119.8	0.25	125
18	4.80	48.00	977	60.4	0.33	110
19	H-S	H-S <sup>2</sup>	718	32.6	0.33	110

<sup>1</sup> Depth to the midheight of the layer

<sup>2</sup> Denotes Half-Space

TABLE 4 VARIATION OF SHEAR-WAVE VELOCITY AND YOUNG'S MODULUS WITH DEPTH AT SECTION 11

Layer Number	Layer Thickness	Layer Depth <sup>1</sup>	Shear Wave Velocity	Young's Modulus	Assumed Poisson's Ratio	Assumed Total Unit Weight
	in.	in.	fps	ksi		pcf
1	1.20	0.60	3005	604.7	0.25	125
2	1.20	1.80	1589	170.2	0.25	125
3	1.20	3.00	732	33.9	0.33	110
4	1.20	4.20	715	32.3	0.33	110
5	1.20	5.40	688	29.9	0.33	110
6	1.20	6.60	677	29.0	0.33	110
7	2.40	8.40	713	32.2	0.33	110
8	2.40	10.80	708	31.7	0.33	110
9	2.40	13.20	708	31.7	0.33	110
10	2.40	15.60	714	32.3	0.33	110
11	2.40	18.00	733	34.0	0.33	110
12	2.40	20.40	612	23.7	0.33	110
13	4.80	24.00	612	23.7	0.33	110
14	4.80	28.80	612	23.7	0.33	110
15	4.80	33.60	660	27.6	0.33	110
16	4.80	38.40	582	21.4	0.33	110
17	4.80	43.20	582	21.4	0.33	110
18	4.80	48.00	660	27.6	0.33	110
19	H-S	H-S <sup>2</sup>	687	29.9	0.33	110

<sup>1</sup> Depth to the midheight of the layer

<sup>2</sup> Denotes Half-Space

respectively. Nineteen layers were used in the inversion process for each site. The thicknesses of the layers ranged from about 1 inch (near the surface) to about 5 inches for subgrade material. To simplify data reduction, the same profiles of thicknesses were used at all sites as follows: six 0.1-ft-thick layers, underlain by six layers each 0.2-ft thick, underlain by six 0.4-ft-thick layers, and a final layer that was assumed to extend to infinity. The more refined the layering selected in inversion, the better determined are the thicknesses of different layers. Also, if only a few layers are assumed (say 3 or 4), it may be impossible to match the theoretical and experimental dispersion curves.

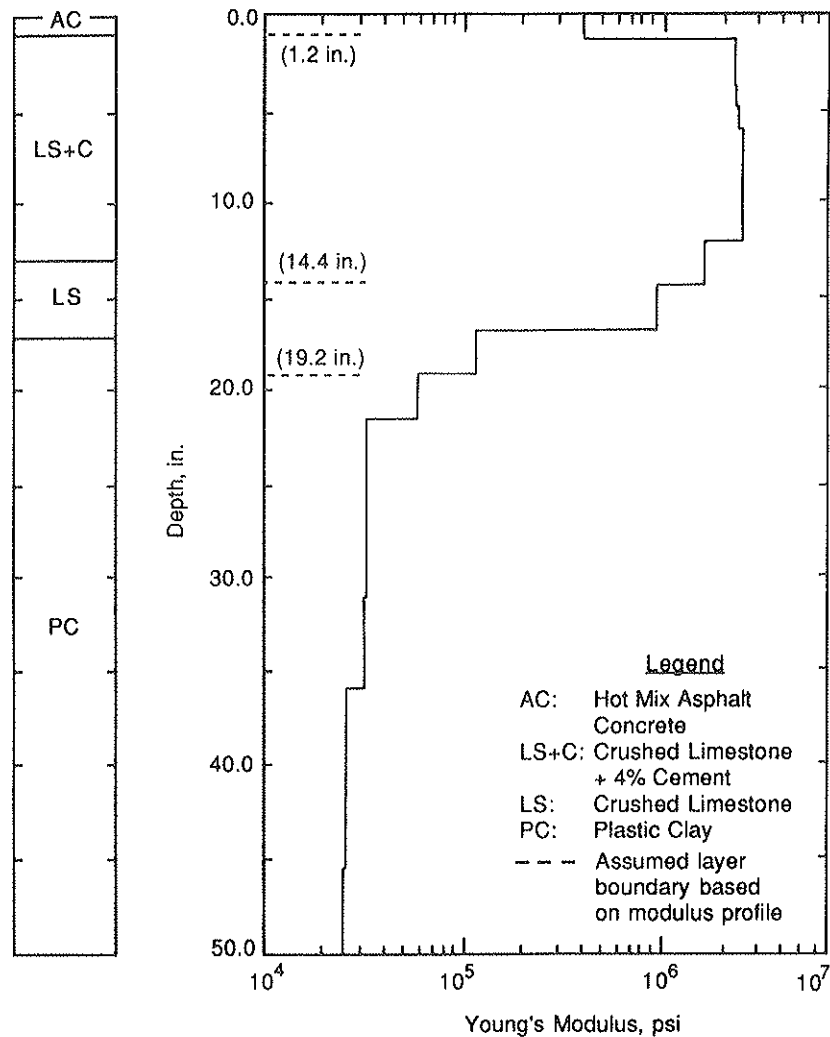
For each site the inversion process consisted of the following steps:

1. The experimental dispersion curve based on the field data was obtained.
2. This experimental dispersion curve was compared with the ones from the previous sites and

- If a similar dispersion curve could be found, the shear-wave velocity profile from that site was used as the starting point to invert the shear-wave velocity profile of the present site;

- Otherwise, a rough inversion using a five-layer system was first performed after which that profile was again inverted using the refined 19-layer system described above.

In the rough inversion process, values of Poisson's ratio and total unit weight of 0.33 and 110 pcf were assumed for all layers. Mis-estimations of Poisson's ratio and total unit weight have minimal effects on the shear-wave velocities obtained by the inversion process (11). However, for the final inversion, the values of Poisson's ratio and total unit weight were modified, based on the shear-wave velocity as shown below (except for the asphaltic-concrete top layer where Poisson's ratio and total unit weights of 0.25 and 125 pcf were used, respectively):



a) Material Profile from Construction Drawings      b) Young's Modulus Profile

FIGURE 6 Composite profile of section 2.

Shear Wave Velocity (fps)	Poisson's Ratio	Total Unit Weight (pcf)
<1000	0.33	110
>1000 and <2500	0.25	125
>2500 (except for AC)	0.15	135

**Young's Modulus**

Based on the shear-wave velocity profiles, Young's moduli at different depths were calculated utilizing equations 7 and 8. The resulting Young's modulus profiles are presented in figures 6 through 14. The total unit weights used in determining Young's moduli are reported in the above table.

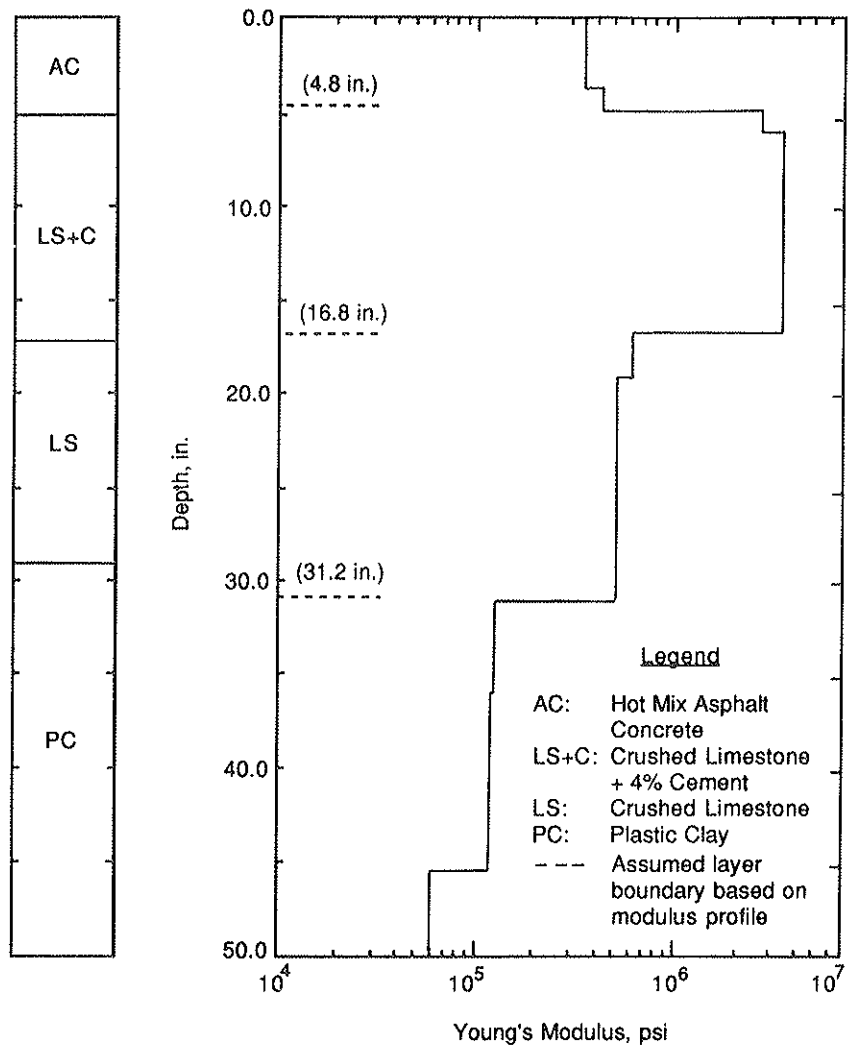
The reason for categorizing total unit weight and Poisson's ratio was that no insight into the nature of the materials at each site was given to the first two authors at the time of data reduction. Based on previous experience with pavement materials, these values of Poisson's ratio and total unit weight seem most reasonably associated with the different materials divided upon the basis of material stiffness (wave velocity).

The material profile of Site 7 was known during data reduction because of initiation of a cooperative project on that section between the time data were collected and the modulus profile was reported.

**DISCUSSION OF RESULTS**

**SASW Tests**

Although the primary intent of this study is to evaluate the sensitivity of the SASW method in determining layer thicknesses, it is interesting and informative to begin by looking at the range in values of moduli determined for similar mate-



a) Material Profile from Construction Drawings

b) Young's Modulus Profile

**FIGURE 7** Composite profile of section 4.



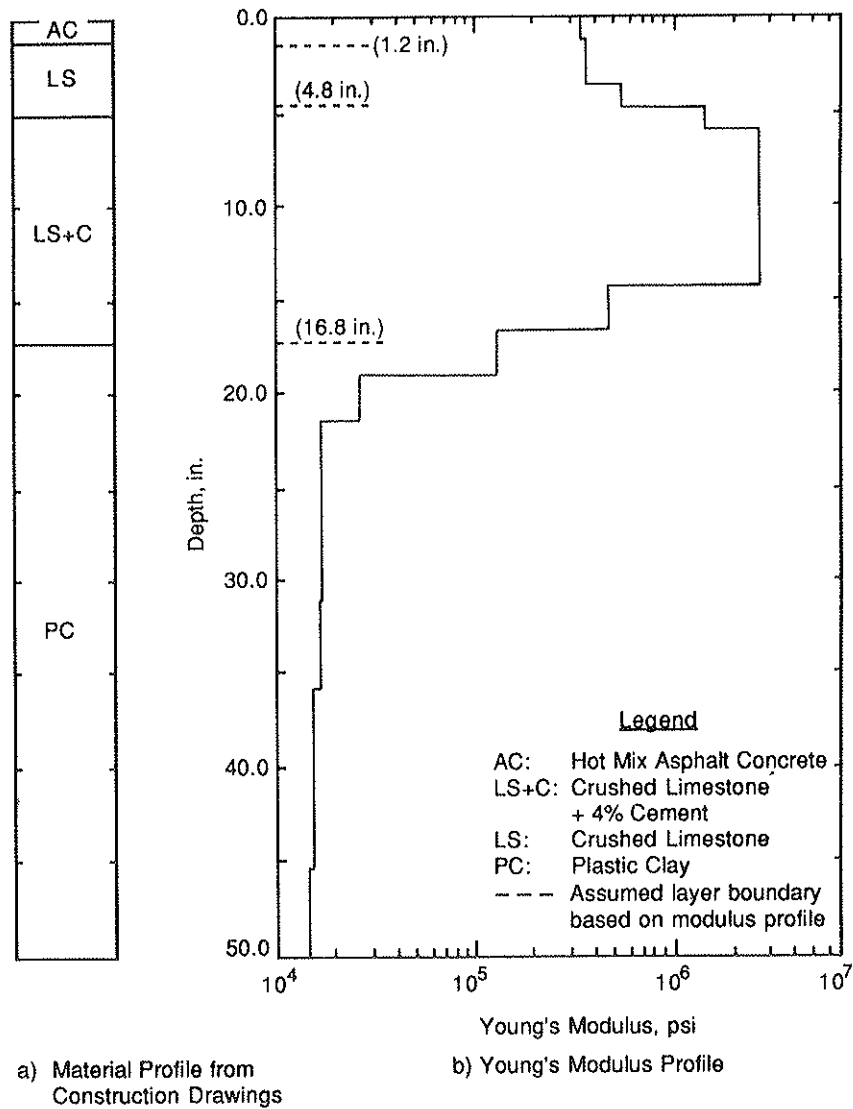


**FIGURE 8** Composite profile of section 7 (material profile was known before inversion).

rials at the nine sites. To simplify this comparison, only average values of moduli near the center of each layer are used. These average modulus values are summarized in table 5.

The modulus of the AC layer ranges from 338 to 1,392 ksi which seems to be a rather large range. However, if Site 9 is deleted from this comparison, the modulus ranges from 338 to 605 ksi, a very reasonable range. The value of the modulus of the AC layer at Site 9 seems unusually high, but additional testing reconfirmed this value. The reason or reasons for this high value are unknown. The results do point out, however, the range in modulus, which can occur even under the carefully controlled conditions at this test facility.

Ranges in moduli for the base, subbase, and subgrade materials are as follows:

- Crushed Limestone: 32–509 ksi
- Crushed Limestone + 4% Cement: 2500–3390 ksi
- Crushed Limestone + 2% Lime: 1200–1340 ksi

- Sandy Gravel: 25–33 ksi
- Sandy Clay 50–51 ksi
- Plastic Clay: 17–34 ksi

Except for the plain crushed limestone base and the sandy clay subgrade, these materials all exhibit reasonable values and ranges in values, with ranges in moduli on the order of two or less. The sandy clay exhibits rather high moduli which are still possible based on the authors' experience. On the other hand, the range in modulus for the limestone base seems too large. The LS base exhibits a very low modulus at Site 9, as if the base did not exist. On the other hand, the limestone base exhibits very high modulus values at Sites 4 and 7. The reason(s) for these low and high modulus values of the LS base is unknown. It is hoped that some of the sites can be cored to determine the precise materials and profiles in the near future.

Prediction of layer thicknesses from the modulus profiles

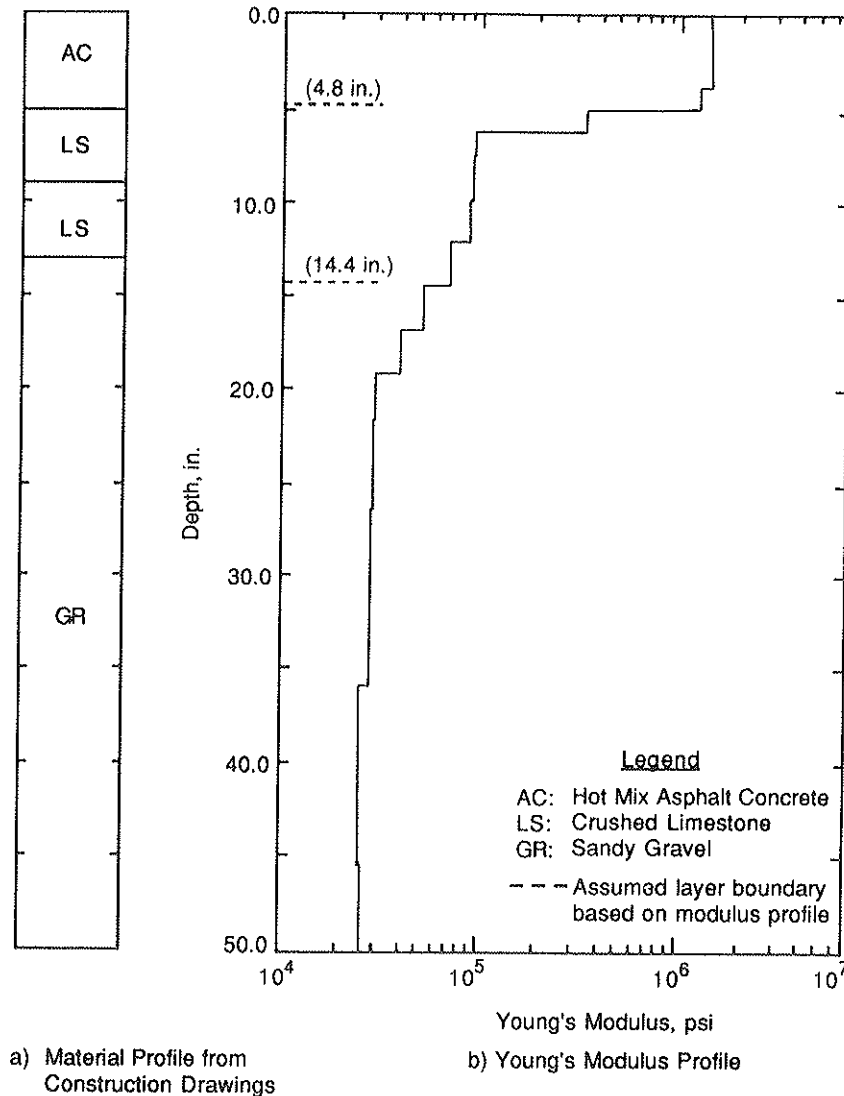


FIGURE 9 Composite profile of section 9.

is quite good at these sites, as summarized in table 6. Depths where the boundaries of different layers were selected are marked on the corresponding Young's modulus profiles presented in figures 6 through 14.

At six sections (Sections 9, 10, 11, 16, 17 and 18) the base layers are subdivided into two sublayers of similar materials simply because of the experimental design procedure employed to determine material types and thicknesses of different layers at each section [see Scrivner and Michalak (12)]. These six sections represent nothing but two-layer pavement systems.

It can be seen in figures 6 through 14 that when the base and/or subbase materials are lime or cement stabilized, determination of thicknesses is quite straightforward because of abrupt changes in the modulus profiles as shown at Sites 4, 16 and 17. However, for other types of base and subbase materials, a transition zone occurs in the modulus profile at layer boundaries which complicates definition of the layer boundaries (such as Site 2 at 19.2-in and Site 9 at 14.4-in). Intuitively, occurrence of this transition zone is logical because

of possible mixing or intrusion of materials on different sides of the boundaries.

One important point when estimating layer thicknesses from modulus profiles is that when the stiffness of two adjacent layers is quite similar, it is not possible to distinguish between these two layers. A good example of this result is the profile of Site 7 where the stiffness of the AC and LS layers is very similar down to a depth of about 5 inches. It is not possible to identify the thickness of the AC layer at this site. From a pavement design standpoint, however, the AC and LS layers will act as one 5-in thick layer with a modulus of about 360 ksi.

The following specific comments can be made about the various profiles:

- At Sites 2, 4, 9, 16 and 17, the thicknesses of the layers estimated from the SASW modulus profiles agree closely with the thicknesses described in the construction drawings. The AC layer thickness is within 0.2 inch, and the base layer

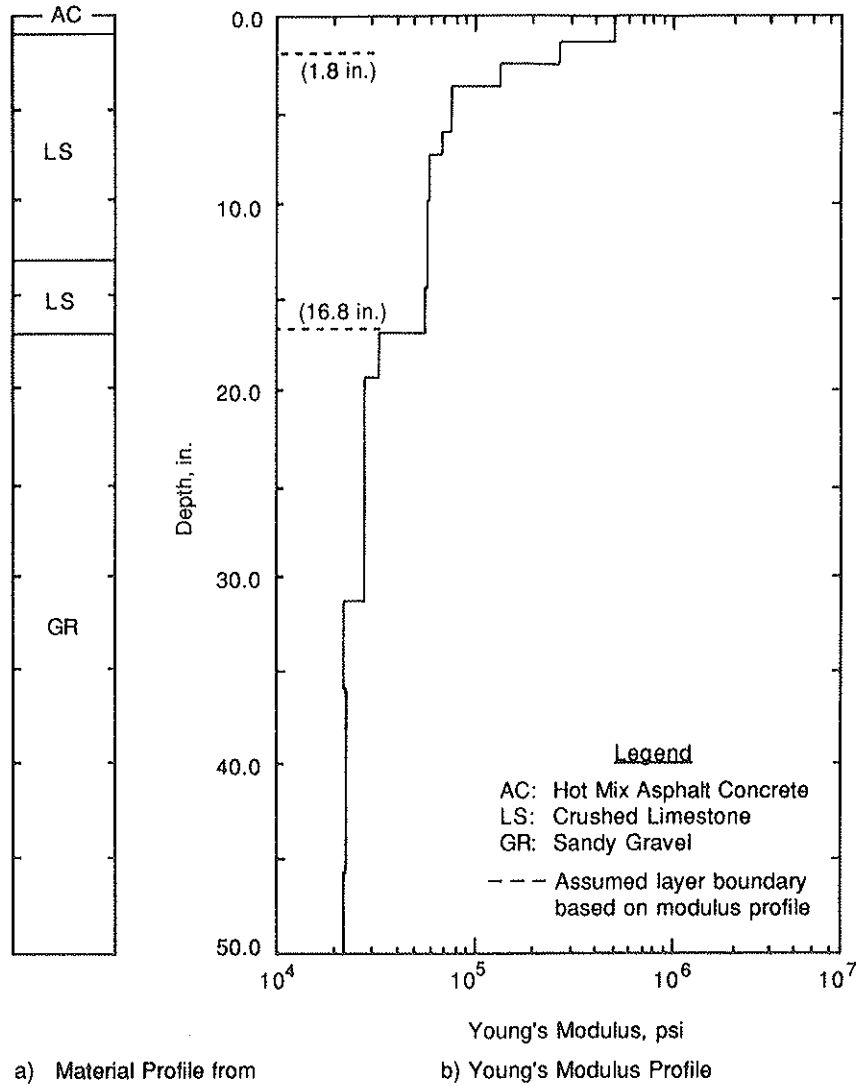


FIGURE 10 Composite profile of section 10.

thickness is generally within about one inch. There is, however, a gradual transition area in the subbase and subgrade layers. These can be due to a gradual change in the property of the subgrade-subbase interface.

- The layer thicknesses at Site 7 were known in advance. However, a transition zone between the subbase and subgrade is detected in the SASW tests, which was unknown but seems possible.

- At Site 9, the modulus of the base layer (LS) is less than similar materials at Sites 4 and 7 and is more similar to the base layer at Sites 2 and 10.

- It seems that the crushed limestone used as a base has a low modulus at Site 10. Once again, a transition zone between the AC and base layers is evident at Site 10. This transition zone seems quite reasonable and thus (probably) represents the actual profile.

- Site 11 has been reported to have an identical profile to Site 10. The SASW profile shows that the layering is quite close for the two sites, but the crushed limestone base at Site

11 is much less stiff than at Site 10. (This matter is also reflected in FWD deflections from the two sites (see table 7). As a result, the depth of the bottom of the base at Site 11 is less well defined than at Site 10. Those sites show that it becomes difficult to select boundaries whenever stiffness contrasts between layers is less than about a factor of 2.

- At Site 18 the boundary of base and subgrade is predicted quite well. However, the boundary between the asphalt and the base layer indicates a gradual change in stiffness, which may or may not exist in the actual profile.

**Falling Weight Deflectometer Tests**

On the same day that the SASW tests were carried out, deflection data were collected using the FWD device. At each section, one FWD test was performed at a nominal load of 9 kips. (Other nominal loads were also applied but were not considered in this study.)

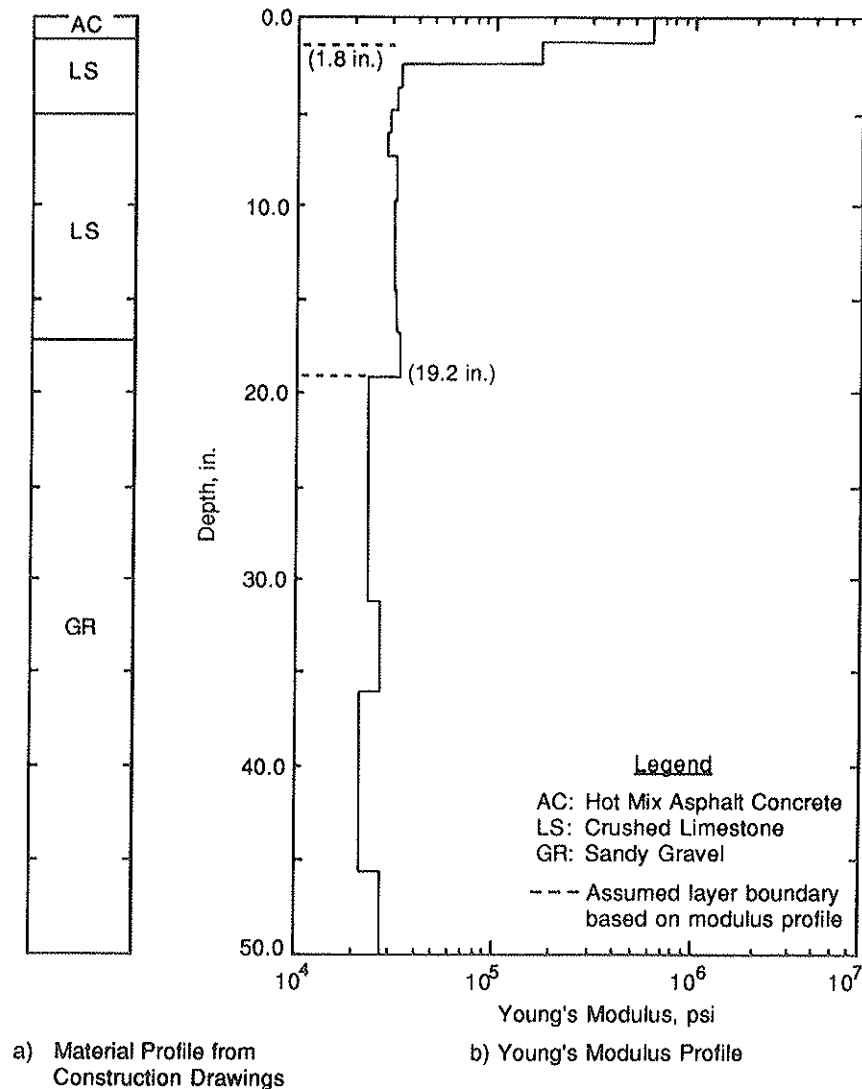


FIGURE 11 Composite profile of section 11.

The actual deflection basins measured in the field are presented in table 7. Preliminary modulus profiles back-calculated by personnel of the Texas Transportation Institute using Program CHEVDEF (13) (see acknowledgements) are reported in table 8. Also included in table 8 is the absolute sum of differences between the measured and calculated deflections. Bush (13) recommends that the absolute sum of the differences should be less than 10 percent for an acceptable fit. It can be seen that in all cases except one (Site 4) the absolute sum of differences is greater than this recommended value. Program BISDEF was also used for back-calculation of moduli. Overall, the absolute sum of the differences between the measured deflection and with BISDEF calculated were similar to those reported for CHEVDEF.

The main reason for the lack of ability in obtaining a better match between the field and theoretical deflection basins can be due to several factors, such as variations in moduli within different layers cannot be considered. A good example is the

subgrade, which consists of two distinct sublayers of fill material and a natural soil layer.

#### Comparison of Moduli from SASW and FWD Tests

In the last section it was mentioned that back-calculated moduli obtained from FWD devices are preliminary because of somewhat large variation between the measured and calculated deflection basins. Therefore, the discussion presented herein is very general in nature.

Moduli of the asphaltic concrete layers obtained by preliminary work on basin-fitting of the FWD data exhibit, in general, greater variation than those of the SASW tests. This is expected because of the lack of sensitivity of the FWD method to the stiffness of the top thin layer, while the SASW method is quite sensitive in this region. It is, however, interesting to

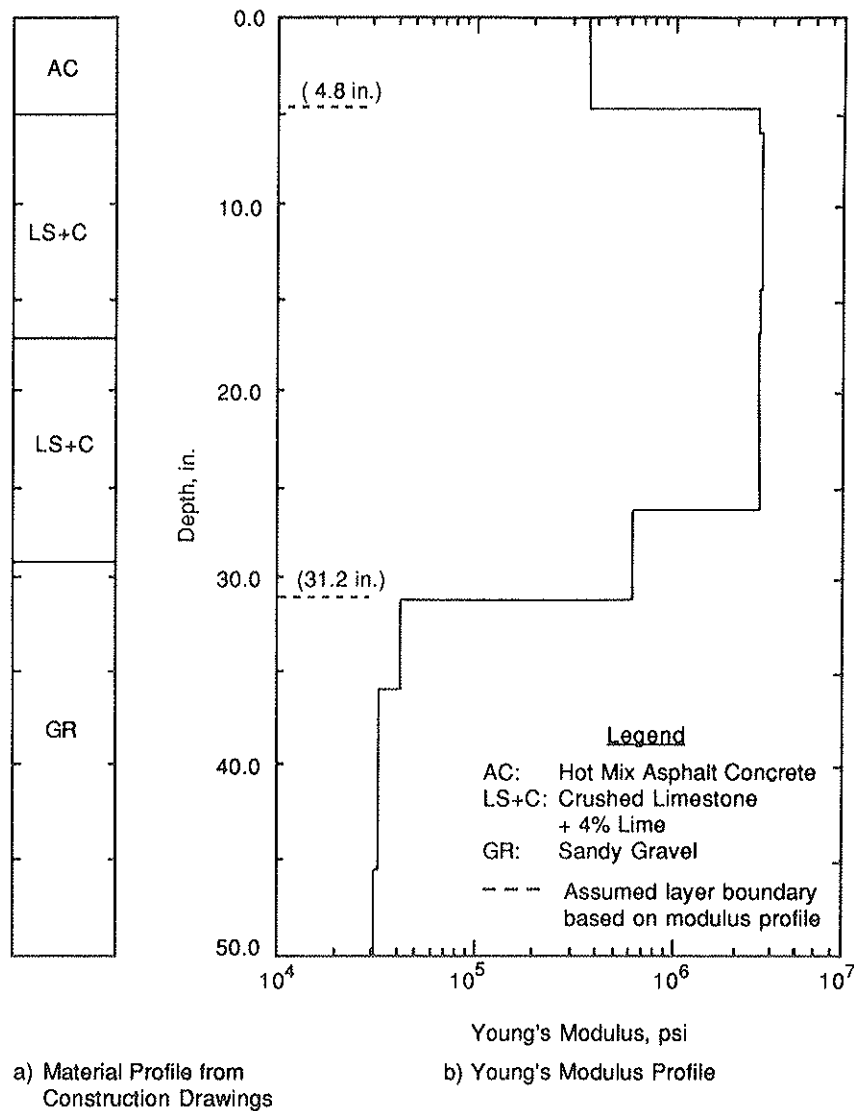


FIGURE 12 Composite profile of section 16.

note that in the FWD results the AC layer at Site 9 exhibits the highest value of modulus, as do the SASW results.

Moduli of the crushed limestone used as the base and/or subbase vary greatly from one section to another as obtained by both methods. At Sites 7 and 10, the moduli are within about 20 percent by both methods. However, for the other sites, modulus values from the two testing methods vary by a factor ranging from 2 to about 20, a poor comparison which is under further study.

Moduli of the cement-stabilized crushed limestone are relatively constant as determined by the SASW tests, with a maximum variation of about 20 percent from the average. A much larger variation in modulus values exists in the FWD results. However, at Sites 2, 4, and 16, the average moduli of this material are within about 15 percent of each other, a good comparison.

Only two sites were tested which have bases of lime-stabilized crushed limestone. The modulus values of this material

do not vary much, as shown in table 5. However, moduli obtained by the SASW method average about 75 percent higher than those obtained by the FWD method.

The three fill materials (sandy gravel, sandy clay, and plastic clay) exhibit the same trends from the two testing methods. The moduli of the plastic clay and sandy gravel are generally within about 25 percent. However, the modulus values of the sandy clay fill from the SASW tests are about twice as large as those obtained by the FWD tests.

Another way of comparing moduli from the two methods consists of inputting the SASW modulus profiles in a layered-theory algorithm (such as BISAR) and determining theoretical deflection bowls. The theoretical deflection bowls can then be compared with the field deflection bowls obtained from the FWD tests. This approach is not very feasible in this study, however, because the SASW modulus profiles are quite shallow. Since the main goal of this project was to obtain the thicknesses of different layers in the upper portion of the

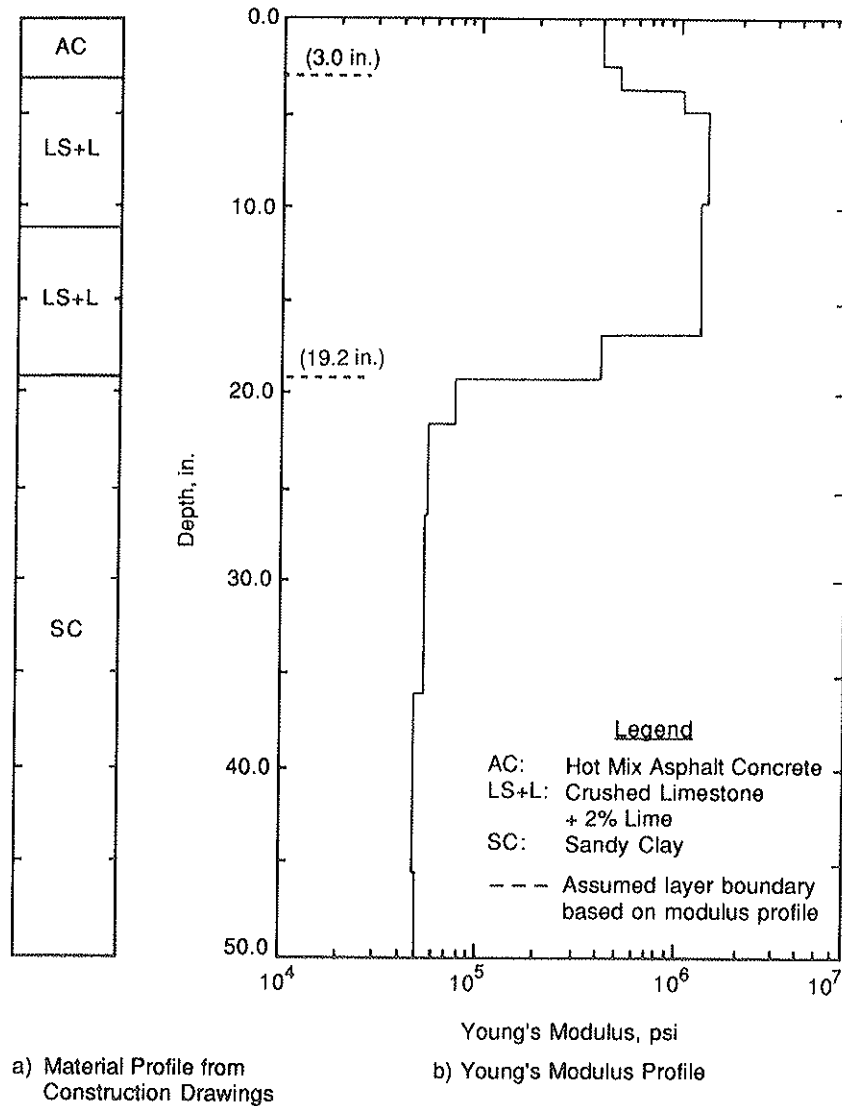


FIGURE 13 Composite profile of section 17.

pavement systems, many layers were placed near the surface, and the moduli were determined accurately to a depth of only about 50 inches.

**CONCLUSIONS**

Overall, moduli and thicknesses determined by the SASW tests seem very reasonable. The accuracy of the layer boundaries determined from the SASW profiles can be further improved by assuming more layers. However, the value of more detailed profiles than presented herein is questionable in the design process. On the other hand, more detailed layer boundaries could be important for construction control, and this result is quite feasible but requires more data-reduction time, which constitutes no problem, and this occurrence should

be studied more rigorously. Most importantly, however, the strength of the SASW method in terms of determining complex stiffness profiles with numerous layers is clearly demonstrated by these tests.

Comparison of modulus values from the SASW and FWD tests at the same sites show several general points. First, moduli of the top pavement layer exhibit less scatter in SASW tests than in FWD tests because of the higher sensitivity of the SASW method to properties in this region of the pavement. Second, moduli of other pavement layers, especially thick, stiff layers such as at Site 16, are generally within about 30 percent by the two types of tests. Third, moduli of the subgrades at six of the nine sites are also within about 30 percent.

Moduli from SASW tests are low-strain moduli. On the other hand, moduli back-calculated from FWD deflection basins may contain manifestations of nonlinear behavior induced by

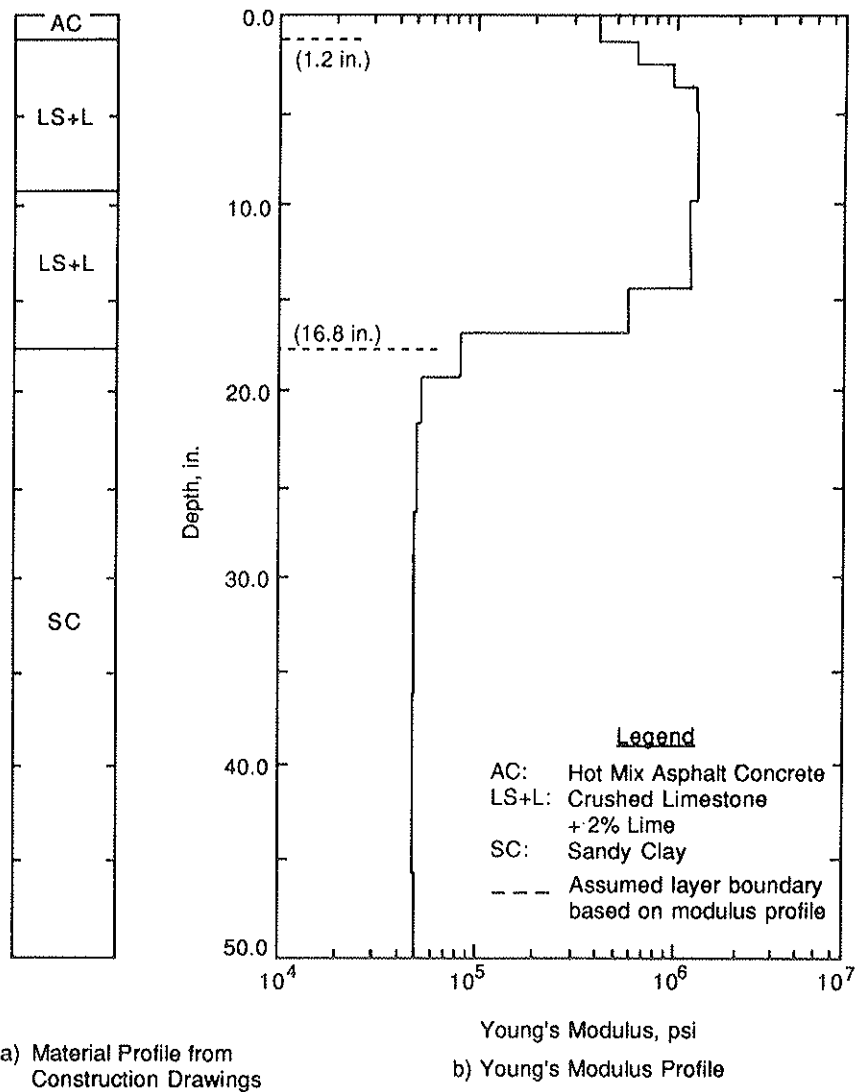


FIGURE 14 Composite profile of section 18.

the heavy loads imparted to the pavement surface. In theory, both tests should yield the same moduli if the boundary conditions for both methods are similar and satisfied properly in the back-calculating procedures. Moduli obtained by the two methods compare well when the predominant pavement layers are thick and stiff. It seems that in these cases both tests are performed in the linear range and the pavement structure is relatively simple.

**ACKNOWLEDGMENTS**

This work was supported by the Texas State Department of Highways and Public Transportation under Contract Number IAC(86-87)0936. The preliminary modulus values obtained from the FWD device were provided by Tom Scullion of the Texas Transportation Institute, whose cooperation is appreciated.

TABLE 5 SUMMARY OF AVERAGE MODULUS VALUES OF MATERIALS DETERMINED FROM SASW TESTS

Section	Average Modulus of Each Material, ksi						
	AC*	LS	LS+C	LS+L	GR	SC	PC
2	409	85	2500	--	--	--	34
4	338	509	3390	--	--	--	33
7	338	362	2727	--	--	--	17
9	1392+	99	--	--	29	--	--
10	500	60	--	--	25	--	--
11	605	32	--	--	25	--	--
16	371	--	2700	--	33	--	--
17	395	--	--	1340	--	51	--
18	395	--	--	1200	--	50	--

\*AC: Hot Mix Asphalt Concrete  
 LS: Crushed Limestone  
 LS+C: Crushed Limestone + 4% Cement  
 LS+L: Crushed Limestone + 2% Lime  
 GR: Sandy Gravel  
 SC: Sandy Clay  
 PC: Plastic Clay  
 + Unusually high value has been confirmed by additional tests

TABLE 6 COMPARISON OF THICKNESSES ESTIMATED FROM SASW TESTS AND CONSTRUCTION DRAWINGS

Section	Thickness from Construction Drawings, in.			Thickness from SASW Profile, in.			Difference in Layer Thicknesses, in.		
	AC	Base	Subbase	AC	Base	Subbase	AC	Base	Subbase
2	1	12	4	1.2	13.2	5.0	0.2	1.0	1.0
4	5	12	12	4.8	12.0	14.4	0.2	0	2.4
7	1	4	12	1.2+	3.6+	12.0	0.2	0.5	0
9	5	8*	--	4.8	9.6*	--	0.2	1.6	--
10	1	16*	--	1.8	15*	--	0.8	1	--
11	1	16*	--	1.8	17.4*	--	0.8	1.4	--
16	5	24*	--	4.8	26.4*	--	0.2	2.4	--
17	3	16*	--	3	16.2*	--	0	0.2	--
18	1	16*	--	1.2	15.6*	--	0.2	-0.4	--

\* Subbase and Base were constructed from the same materials.  
 + AC Layer and Base have about the same modulus and would be interpreted as one layer with a thickness of 4.8 in. if the material profile was never known.



TABLE 7 DEFLECTION BASINS MEASURED AT TTI PAVEMENT TEST FACILITIES

Section	Load, lbs	Deflection, mils						
		Sensor Number*						
		1	2	3	4	5	6	7
2	9480	6.8	5.7	4.7	3.9	3.0	2.4	1.8
4	9392	3.2	2.3	2.3	2.0	1.7	1.5	1.3
7	9376	11.5	6.2	5.5	4.6	3.8	3.0	2.5
9	9368	9.3	5.9	3.6	2.4	1.7	1.3	1.2
10	9432	16.2	7.6	4.1	2.9	2.2	1.8	1.4
11	9176	19.7	7.6	3.6	2.5	1.9	1.6	1.2
16	9288	2.1	1.4	1.4	1.3	1.1	1.0	0.9
17	9384	6.3	5.2	4.3	3.5	2.8	2.2	1.8
18	9392	5.0	4.2	3.7	3.1	2.6	2.2	1.7

\* Sensor Number 1 was located directly under the load and the other 6 sensors were placed one foot apart.

TABLE 8 SUMMARY OF MODULUS VALUES BACK-CALCULATED FROM FWD TESTS

Section	Average Modulus of Each Material, ksi							
	AC*	LS	LS+C	LS+L	GR	SC	PC	ASD <sup>a</sup> , percent
2	947	23	3119	--	--	--	24	18.7
4	609	87	4491	--	--	--	32	4.1
7	864	293	797	--	--	--	19	19.6
9 <sup>b</sup>	1000	100	--	--	23	--	--	61.8
10	885	69	--	--	27	--	--	24.8
11	475	65	--	--	32	--	--	25.4
16	302	--	2125	--	46	--	--	12.6
17	570	--	--	851	--	22	--	35.0
18	320	--	--	631	--	21	--	24.6

<sup>a</sup> ASD denotes Absolute Sum of Percent Difference between the measured and backcalculated deflection basins.

\*AC: Hot Mix Asphalt Concrete  
 LS: Crushed Limestone  
 LS+C: Crushed Limestone + 4% Cement  
 LS+L: Crushed Limestone + 2% Lime  
 GR: Sandy Gravel  
 SC: Sandy Clay  
 PC: Plastic Clay

<sup>b</sup> Modulus values for Site 9 backcalculated by personnel at The University of Texas at Austin

## REFERENCES

1. S. Nazarian and K. H. Stokoe, II. *In Situ Determination of Elastic Moduli of Pavement Systems by Spectral-Analysis-of-Surface-Waves Method (Practical Aspects)*. Research Report 368-1F. Center for Transportation Research, The University of Texas at Austin, 1985.
2. S. Nazarian and K. H. Stokoe, II. *In Situ Determination of Elastic Moduli of Pavements Systems by Spectral-Analysis-of-Surface-Waves Method (Theoretical Aspects)*. Research Report 437-2. Center for Transportation Research, The University of Texas at Austin, 1986.
3. B. O. Hardin and V. P. Drnevich. Shear Modulus and Damping in Soils: Measurement and Parameter Effects. *Journal of the Soil Mechanics and Foundations Division*, ASCE, Vol. 95, No. SM6, 1972, pp. 602-624.
4. R. D. Barksdale and R. G. Hicks. Material Characterization and Layered Theory for Use in Fatigue Analysis. In *Special Report 140: Structural Design of Asphalt Concrete Pavements To Prevent Fatigue Cracking*, HRB, National Research Council, Washington, D.C., 1973, pp.20-49.
5. I. Sanchez-Saliner. *Analytical Investigation of Seismic Methods Used for Engineering Applications*. Ph.D. dissertation. The University of Texas at Austin, 1987.
6. J. C. Sheu, I. Sanchez-Saliner, J. M. Roesset, and W. R. Hudson. *Investigation of Variables Affecting In Situ Determination of Elastic Moduli of Pavement Systems by Surface Wave Method*. Research Report 437-3F. Center for Transportation Research, The University of Texas at Austin, November 1986.
7. W. T. Thomson. Transmission of Elastic Waves through a Stratified Solid Medium. *Journal of Applied Physics*, Vol. 21, 1950, pp. 89-93.
8. N. A. Haskell. The Dispersion of Surface Waves on Multi-layered Media. *Bulletin of the Seismological Society of America*, Vol. 43, No. 1, 1953, pp. 17-34.
9. S. Nazarian, K. H. Stokoe, II, and R. C. Briggs. Nondestructively Delineating Changes in Modulus Profiles of Secondary Roads. In *Transportation Research Record 1136*, TRB, National Research Council, Washington, D.C., 1987, pp. 96-108.
10. S. Nazarian, K. H. Stokoe II, and W. R. Hudson. Use of Spectral-Analysis-of-Surface-Waves Method for Determination of Moduli and Thicknesses of Pavement Systems. In *Transportation Research Record 930*, TRB, National Research Council, Washington, D.C., 1983, pp. 38-45.
11. S. Nazarian. *In Situ Determination of Elastic Moduli of Soil Deposits and Pavement Systems by Spectral-Analysis-of-Surface-Waves Method*. Ph.D. dissertation. The University of Texas at Austin, 1984.
12. F. Scrivner and C. H. Michalak. *Linear Elastic Layered Theory as a Model of Displacements Measured within and beneath Flexible Pavement Structures Loaded by the Dynaflect*. Research Report 123-25. Texas Transportation Institute, Texas A&M University, College Station, Tex., 1974.
13. J. A. Bush. *Nondestructive Testing for Light Aircraft Pavements, Phase II, Development of Nondestructive Evaluation Methodology*. Report No. FAA-RD-80-9-II. U.S. Army Corps of Engineers, Vicksburg, Miss., 1980.

---

*Publication of this paper sponsored by Committee on Strength and Deformation Characteristics of Pavement.*